RETROFITTING A JET DRIVEN UAV TO FORM A MULTI-PURPOSE TEST PLATFORM

Dániel Teubl[1], Thando B. Sissing[1] & Mirko Hornung[1]

[1]Chair of Aircraft Design, Technical University of Munich

Abstract

The testing and evaluation of a custom part or new software requires the use of an easily operable unmanned aerial vehicle. For this goal, the retrofitting process of a high-end, remotely controlled, jet-driven, scaled glider is presented. The purpose of the overall work is to utilize an off-the-shelf airframe to support multiple research projects. This paper lists the requirements for the retrofitted airframe, along with a possible selection of currently available system components such as autopilot or remote-control modules. The overall design of the system and the major subsystem designs are presented. Laboratory tests, a range test and flight tests are carried out to validate the results of the integrated system.

Keywords: UAV, Sensor systems, Px4, system integration

1. Introduction

Various Unmanned Aerial Vehicles (UAVs) with different Maximum Take-off Mass (MTOW) classes are in use at the Chair of Aircraft Design (LLS). Examples of this, are the 1–2kg MTOW Rapid Evaluation Class (REC) vehicles used for teaching, practice and short missions, in addition to performing quick evaluation of custom parts, or new software. Such vehicles are described in [1, 2]. In the 5–15kg MTOW range, a series of in-house developed Vertical Take-off and Landing (VTOL) UAVs are used for design evaluation and flight performance testing [3]. An external VTOL is regularly used for propeller noise emission modelling and evaluation [4]. In the 15–25kg MTOW range, a DG-800 S scaled UAV is utilized for pilot training and data collection for system identification purposes [5, 6]. Above 25kg MTOW, the T-FLEX [7] and P-FLEX technological demonstrators are used for scientific research [8, 9, 10].

In the research and development fields, each UAV weight class has its benefits and limitations. Having access to smaller airfields close to one's workplace, encourages the use of smaller and lighter UAVs.

The main limitation of 1–2kg MTOW UAVs is the small payload capacity, as well as low Signal to Noise Ratio (SNR) and unknown or changing aerodynamic characteristics. However, since these are easy to operate, they are a perfect candidate for REC vehicles.

The 5–15kg MTOW UAVs have better payload capabilities as well as improved SNR. Commerciall off-the-shelf (COTS) UAVs have a wide range of performance characteristics. They are designed and built for specific mission profiles while keeping the operation effort relatively low. There is a need for such a platform at LLS.

Above 25kg MTOW, custom built UAVs or Scaled Flight Demonstrators (SFDs) are used to validate new technologies such as active flutter suppression [11, 7] or serve multiple research initiatives [11, 8, 12]. These platforms can yield exceptional results in a cost effective and safe way in comparison to general aviation. However, the design, manufacturing and operation of these systems in addition to their infrastructure are too costly for a single university institute.

Within the 15–25kg MTOW range, some of the advantages of the lower and higher MTOW classes can be combined. In most cases, the UAV can be operated by the pilot only. Additional personal

such as a flight test engineer or flight test manager along with a suitable Ground Control Station (GCS) can be used to minimize the Plan-Do-Study-Act (PDSA) feedback cycle between flights. The payload capacity with in these systems allows the use of complex On-Board Computers (OBCs) with additional sensor systems. Due to the availability of many COTS UAVs in both the professional and semi-professional categories, the use of a custom design can be avoided by retrofitting a suitable airframe. Such a suitable COTS UAV is the DG-800 S from Carf-Models [13].
The main objective of this paper is to present the current status and capabilities of the DG-800 S. Each sub-system will be described in-depth along with the overall system layout and major design choices. System integration and ground test results are presented to highlight the capabilities of the system.

2. Related Work

This section describes different COTS equipment, such as autopilot systems, Remote Control (RC) systems and autopilot companion or on-board systems used in small scale flight testing. Along with these, a brief introduction is given about the flight test capabilities of the LLS.

2.1 Fixed-wing Flight Test Platforms

Table 1 shows the recently used fixed-wing flight test vehicles at LLS along with an other research UAV used at the Technical University of Munich.

Table 1 – Comparison of Flight Test Vehicles

MTOW [kg]	Design Speed[m/s]	Flight Time [min]	Wingspan [m]	Length [m]	Payload [kg]
2.7 [1]	17	15	1.63	1.17	-
1.0 [2]	16	10	1.4	0.925	0.15
65 [7]	50	15	7.07	3.42	-
20 [6]	50	6-15	6.0	2.35	2
1-2 [14]	20	20	1.3	0.83	0.12

A mobile GCS were developed at LLS to support flight testing activities with the T-FLEX [7] demonstrator. The same GCS is actively reused with other systems. A live video stream of the flying UAV can be accessed in the GCS via a ground based tracking system. The tracking system uses the actual Global Positioning System (GPS) coordinates of the UAV.

2.2 Autopilot Hardware and Applications

The following table 2 presents a comparison of common autopilot hardware used with open source autopilot software. These are some of the autopilots which were found to be compatible with the current system and have a large online support community. Important design considerations where used as a basis for comparison such as integrated sensors, connectivity and size as these were th main factors for choosing one component over another.

2.3 Remote Control Systems

A few RC transmitters are compared in table 3, these are more extensively used at our Institute. Both JETI Model Duplex Radio System (JETI) and PowerBox systems have their compatible telemetry sensors and power distribution modules. Scripting support and open logfile format where features found to be useful when creating custom data inputs or integrating data from the RC into the rest of the system for analysis.
The LoRa [27] capable FrSky Tandem [28] series, or other ExpressLRS [29] compatible radio modules are not listed due to the author's lack of experience with these systems.

Table 2 – Comparison of Autopilot Hardware. The abbreviations used in the table are the following. b: barometer, m: magnetometer, p: pitot tube sensor, c: CAN, s: SPI, a: ADC, pp: PPM, sb: S.BUS, ds: DSM, cp: CPPM, g: GPS, ag: Accel/Gyro, e: ethernet, u: UART, us: USB

Autopilot	Sensors	Interfaces	Dimensions(mm)	Weight(g)
CubePilot Cube Orange [15]	b,m,ag	c, s, a, pp, sb, ds, g, u	94.5x44.3x22.3	-
Holybro Pixhawk 4 [16]	b,m,ag	c, s, a, pp, sb, ds, cp, g, u	44x84x12	15.8
Holybro Pixhawk 5X [17]	b,m,ag	c, s, a, pp, sb, ds, g, u, e	52.4x21x103.4	74
Holybro Pixhawk 6C [18]	b,m,ag	c, a, pp, sb, ds, cp, g, u	84.8x44x12.4	59.3
Sky-Drones AIRLink [19]	b,m,ag,p	c, s, a, pp, sb, ds, g, u, e, us	61x103x37	198
ArduPilot Mega [20]	b	a, pp	70.5x45x13.5	31
OpenPilot Revolution [21]	b,m,ag	s, a, pp, sb, g, u	36x36x12	-
TauLabs Sparky2 [22]	b,m	c, pp, ds, u	36x36	13.5

Table 3 – Comparison of RC Transmitters

feature	PB Core [23]	Jeti DC-16 II [24]	JETI DS-24 [25]	FrSky [26]
No. channel	24	24	24	24
No. 2.4Ghz receivers	4	2	2	1
No. 900Mhz receivers	-	1	1	-
scripting support	-	Lua	Lua	lua
open logfile format	no	yes	yes	yes

2.4 On-Board Computers

Table 4 presents a comparison of the characteristics and performance of OBCs that can used with autopilots. These OBCs were found to have a large use base and online community support. In addition this they have onboard Wi-Fi (Wi-Fi) or the capability to have COTS Wi-Fi easily integrated into them. There is also the possibility of Universal Serial Bus (USB) connection to the Autopilot for data transfer. Most of these are also able to run a linux-based operating system.

Table 4 – Comparison of On-Board Computers

Device	Processor	RAM (GB)	Dimensions (mm)	Weight(g)
Pixhawk RPI CM4* [30]	Quad-core ARM Cortex-A72	8	58x112x24.8	80
Auterion Skynode* [31]	ARM Cortex-A53 Quad Core	4	58x110x31.5	188
Raspberry Pi 5 [32]	Quad-core Arm Cortex-A76	8	56x88x16	46
Odroid-M1S [33]	Quad-core ARM Cortex-A55	8	65x90x16	52
Jetson Nano [34]	Quad-core ARM Cortex-A52	4	79x100x30.21	138
Jetson Xavier [35]	8-core NVIDIA Carmel Armv8.2	32	209x223x134	1548

*Integrated with autopilot

2.5 Object Tracking Hardware

Table 5 gives a brief overview of sensors typically integrated into gimbal systems. Some important factors such as the integrated sensors, camera resolution as well as size were used as a basis for comparision. This is due to the limited payload capacity of the UAV.

Table 5 – Sensor systems for object tracking. The abbreviations used in the table are the following: r: rgb camera, i: infrared camera, t: thermal camera, l: lidar

Gimbal	Sensor	RGB Resolution	Dimensions (mm)	Weight(g)
Optroxa GMB 600 [36]	r,i,t	1440x1080	83x98x125	600
GSG 201 [37]	r,i,l	1920x1080	323x200x200	3500
Rpi Picamera [38]	r	3280x2464	80x80x90	95
USG-405 [39]	r,i,l	1920x1080	83x98x125	3100
TAROT T2-2D [40]	r	3840 x 2160	99x95x105.6	278
Siyi A8 [41]	r	4096 x 2160	55x55x70	95

3. Requirements

Based on the author's experience with previous flight-test platforms, a set of requirements were collected before the retrofitting process. The requirements presented here are the ones with the most influence on the system design. Thus only a subset of the original requirements are listed.

Requirements:

1. The platform shall be operable on a RC model airfield.
2. The platform shall be operable by one person.
3. The RC system shall be compatible with a scripting language.
4. The RC system shall produce a parsable log without the need for a third-party graphical tool.
5. The actual power consumption data shall be available from each power source during operation and in the logs.
6. The platform shall use a standard COTS avionics system.
7. The platform shall use a Flight Control Computer (FCC) system, which is widely accepted in the research community.
8. The flight control system shall work independently from the additional measurement systems.
9. The platform shall use a high-bandwidth, long-range telemetry system.

Satisfaction of Req. 1 will allow less constrained operation of the system, due to the limited availability of additional persons involved with operation on top of the flight crew. Conducting operation around sunrise or sundown in calm weather conditions would be dependent on the flight test team only.
Req. 2 is chosen to minimize the operational burden of the system. Normal flight operation at LLS consists of one or two pilots, an operator and an engineer. If there is a need the pilot can operate the whole system alone, while the other persons can focus more on the actual experiment and data analysis. With that, information feedback cycles can be shortened. Easy operation of a system will ensure a more frequent conduction of experiments, thus resulting in even shorter feedback cycles.
Req. 3 is set to allow high level of user configurability of the RC system. Systems which can run custom user applications allows higher configuration and better user experience compared to other systems. Functions like custom signal injection can be implemented without reconfiguration of the autopilot system, or used in a system which does not have autopilot capabilities [6, 2]. This allows better separation of system functionalities and testability.
The datalog created by the RC system contains valuable information about the reception quality of its radio. Synchronization of the RC radio's data to the other data sets collected during a mission, allows an easier and better data analysis experience. To make the synchronization process automatic, the datalog of the RC system shall be automatically convertible to csv like format as stated in Req. 4.

In case the system requires multiple voltage levels or multiple batteries due to redundancy, all standalone batteries shall be monitored as stated in Req. 5. This allows live monitoring of each individual battery during operation, and the availability of the stored data for post processing.
Req. 6 and Req. 7 will allow easier comparison of the system's results with other UAV results due to the similarity of collected data and it's quality. Shared FCC would allow easier reuse of control or identification algorithms between platforms. Using a COTS system will drastically reduce development and integration time as well.
Req. 8 allows the separation of autopilot and mission oriented functionalities as well as reducing hardware and software coupling. It would make possible to update or change the autopilot system without compromising other system functionalities.
Telemetry data is essential for live monitoring and control of a UAV. The availability of high bandwidth telemetry stream over long operational range as stated in Req. 9. This allows smoother operation and precise feedback about the state of the system. Moreover, it makes it possible to use recursive algorithms to generate similar views of the system during flight as normally used during analysis.

4. Systems Design

The following section explains the main considerations for the design of each subsystem. The characteristics of each subsystem is accompanied by a short explanation of the part selection. Figure 1 illustrates the major connection between subsystems.

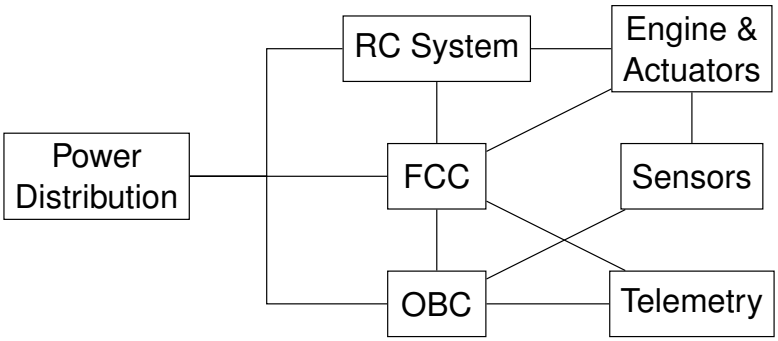

Figure 1 – System Component Diagram

4.1 Fixed-wing Unmanned Aerial Vehicle

The DG-800 S was previously used at the Institute to test various custom sensors [6, 2] or assist in the development of hardware and methodology [5, 42]. In addition to this, it was used for pilot training during the Flexop [9] and Flipased [10] projects. Figure 2 shows the DG-800 S at the FMSG Herrieden Stadel [43] model airfield.
The size, low complexity and capacity payload area of the DG-800 S allows it to be a good candidate to support multiple research projects. Its wing-span and propulsion system make it unsuitable for operation at the local LLS airfield. This is due to its required take of distance, runway surface requirement as well as flight regulations. However, its operation is possible on other model airfields, thus it satisfies Req. 1. Table 6 presents a few main parameters of the DG-800 S, which satisfies Req. 2 even with normal configuration.

Figure 2 – DG-800 S UAV

Parameter	Value	Unit
Wingspan	6.0	m
Length	2.35	m
Wing area	1.3	m^2
Max takeoff weight	20.3	kg
Max payload	2	kg
Design speed	50	m/s
Flight duration	6-15	min

Table 6 – Main Parameters of the DG-800 [5]

4.2 Remote Control System

The remote control system of the aircraft was changed from the PowerBox CORE [23] system to the JETI [24] system. This change took place due to the increase in available functionality and performance.

4.2.1 Design Choice Motivation

During the rebuild-process of the P-FLEX demonstrator [7], an in-depth range test campaign was conducted with three different RC radio systems. Namely, the Graupner radio System (Graupner) [44], PowerBox CORE [23] and two JETI systems [24, 25]. During that range test campaign, both the 2.4Ghz and the Next Generation 900Mhz receiver configuration of the JETI system outperformed the others systems.

The JETI system supports a Lua programming interface, which allows access to hidden system information such as the Received Signal Strength Indicator (RSSI) values, user interface modification or implementation of complex logical functionalities such as signal injection applications. None of the other systems, investigated allowed this level of integration. Using this system satisfies Req. 3.

The system log produced by the JETI system is stored in ASCII format, and is easily understandable without a third-party graphical application. This allows the integration of the logs created by the RC system with the logs created by the other subsystems, thus satisfying Req. 4. As a result a more elaborate mission performance analysis can be made. From the investigated systems, this was the only one with the potential of this level of analysis.

Both JETI and system have their own power and Pulse Width Modulation (PWM) signal distribution units such as the Central Box or PowerBox. Fortunately, both distribution systems are compatible with the other types of RC systems. They also share the same base functionalities as well. However, active output voltage modulation function is only available on the Central Box. Since the Central Box 310 module has enough input output capabilities, in addition to its output modulation function, it was selected for the system.

4.2.2 Components and Layout

The main components used are the CB310, two Rex3 modules, and a RSATNG900 module. Since no custom parts are used for the RC system, the recommended connection and layout was followed. Using this configuration satisfies Req. 6.

4.3 Flight Control Computer

Figure 3 illustrates a Pixhawk 4 FCC, which is used within the system. This FCC was chosen because it was already in use in other UAV research projects at LLS and is compatible with the users currently at the institute. The choice of Px4 also satisfies Req. 6 and Req. 7.

It is optimized for Px4 autopilot [45] software, but is also supports ArduPilot [46] as well. Both software have a large support community, are well documented, and have many of their functions extendable or modifiable via coding languages such as Python and C++. The Pixhawk 4 is used with Px4 autopilot within the DG-800 S. Px4 provides preliminary processing of the data from sensors, and PWM

signals to operate servomotors. During flight, the sensors in use are a GPS sensor, barometer, accelerometer/gyroscope, magnometer, and indicated airspeed sensor (Pitot tube). Data is propagated to the rest of the system via the connected telemetry and USB cables.

Figure 3 – Pixhawk 4 Autopilot [16]

4.4 Power Distribution

The CB310 module supports two 2S Lithium polymer (Li Po) batteries for redundancy. The Electronic Control Unit (ECU) and the turbine require a 3S Li Po battery for operation. The OBC requires a stable $5V_{DC}$, with sufficient current. The Px4 can be operated from the 2S and 6S batteries via the PMU modules.

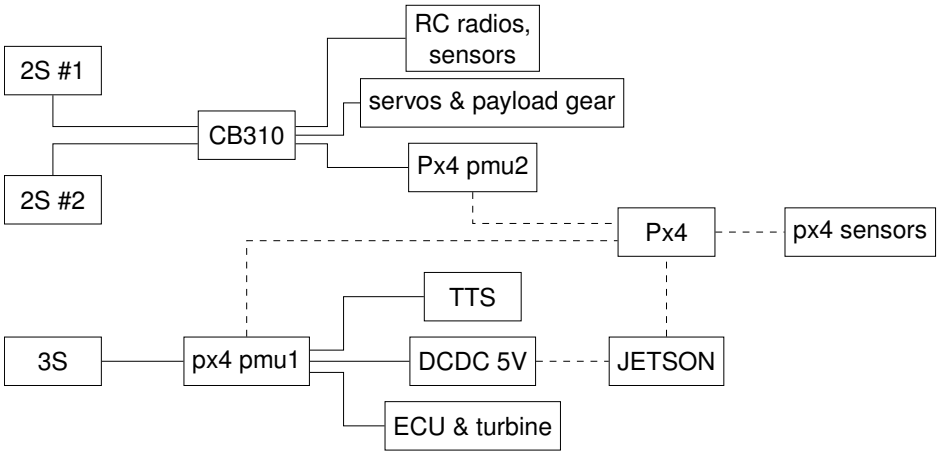

Figure 4 – Power Distribution Layout (dashed lines indicate $5V_{DC}$)

Figure 4 shows the main power connections of the designed system. All the RC components, the servo motors and the monitoring systems are powered by the CB310 module. The OBC, the propulsion system and the object tracker are powered by the 3S battery. The Px4 module is powered from multiple sources, and it powers the sensors and telemetry modules connected to it. There is no need for a sophisticated power distribution system, as each system delivers sufficient power to the components attached to it.
The requirement for the power source measurement system Req. 5 is satisfied for the flight control batteries via the CB310 module. For the ECU and payload battery, a Px4 PMU module is used for monitoring the available power.

4.5 Telemetry System

In previous flight-test campaigns with the T-FLEX/P-FLEX demonstrators, the control and monitoring functionalities were separated due to functional and safety reasons. This separation introduced some additional complexity, but increased the monitoring capabilities. Similar separation is done with this system.
One of the telemetry systems used is the RFDesign 868Mhz Ultra Long Range Radio Modem [47] (RFD 868) telemetry module. The other is a high quality Wi-Fi module from Doodle Labs [48] with a long range ground control antenna. The RFD 868 module will be used for operation control via the

QGroundControl software. The Wi-Fi module is used for monitoring. In case of stable reception, The Wi-Fi based telemetry can be used for operation control, while the RFD 868 system acts as a backup. The Wi-Fi based telemetry system fully satisfies Req. 9.

4.6 On-Board Computer

Figure 5 below illustrates a Jetson Nano, which is used within the system as an OBC. The main reason for this design choice was its size, cost and processing capability at the time the software development process began. In addition to these, it can run an Ubuntu operating system, allowing the use of the same configuration on the development and the deployment environment. As it will be used for image processing, the possibility for further leveraging its GPU to increase processing speed was also considered. The Jetson Nano is also capable of running the software used to interface with the FCC. Its main purpose within this system is used to run the object tracking software, control the gimbal, package data from hardware components, and route data throughout the system.
Using a Jetson Nano as OBC satisfies Req. 6 and Req. 8.

Figure 5 – Jetson Nano (OBC) [34]

4.7 Target Tracking System

The Target Tracking System (TTS) consists mainly of a two axis (pan and tilt) gimbal, a small video camera and video transmitter. These components were chosen as they are cheap and easily replaced as the gimbal is located at the nose of the UAV where there is a possibility of it being damaged. In addition to this the tracking system had to be as small and as light as possible due to the payload and space limitations of the system.
For the current application the Siyi A8 [41] was selected, due to it's compact size and fully integrated camera and gimbal system.

4.8 Actuator Monitoring

The servo motors of the ailerons and flaps were previously retrofitted with Actuator Control and Monitoring Units (ACMUs). The detailed configuration and results of this process are mentioned in [2]. A broad overview of the ACMU and its capabilities is described in [49].
An USB connection has been established between each ACMU and the OBC. The active connection allows live data streaming and visualization during operation. Other functionalities like firmware update, configuration update or log file retrieval are available via the USB interface as well.
The data sets collected from the individual ACMUs are synchronized to the Px4 data set using the reference PWM signals. The PWM signals are converted to relative angles by matching their offset and amplitude to the respective servo shaft angle measurements. This method provides a good basis for behavior analysis, but requires external angle measurement for exact matching.

5. Results

This section describes the integrated state of the system, along with the laboratory, range test and flight test results.

5.1 Integration

The integration of the system was executed iteratively. First, a subsystem was assembled and tested outside the fuselage. Then part by part, it was placed into the fuselage with long enough cabling. When a good position was found for a part, it was configured and secured in place. The respective cables and connections were trimmed to ideal length only, all the connection of the part were established and configured. The same process is done for each part.
This approach allows one to do an almost continuous integration of the different subsystems. This was found to be advantageous in that it allows easier familiarity with new systems, flexible arrangement of parts and cables for a longer duration during integration, as well as the testing and readjustment of functionalities and subsystems within the UAV.
Figure 6 shows the avionics bay with and without the avionics plate prototype. The avionics plate was designed and integrated in a way, that makes it easily removable and interchangeable with other layouts. To achieve this, the number connections between the avionics plate and the rest of the aircraft is minimized.
On Fig. 6a, the following part's of the system are highlighted: the Px4 autopilot (1), the 3S battery connection (2), the 2 2S battery connections (3), the GPS module (4), the RFD 868 telemetry radio (5), the OBC (6) and the Wi-Fi module with its antenna (7).

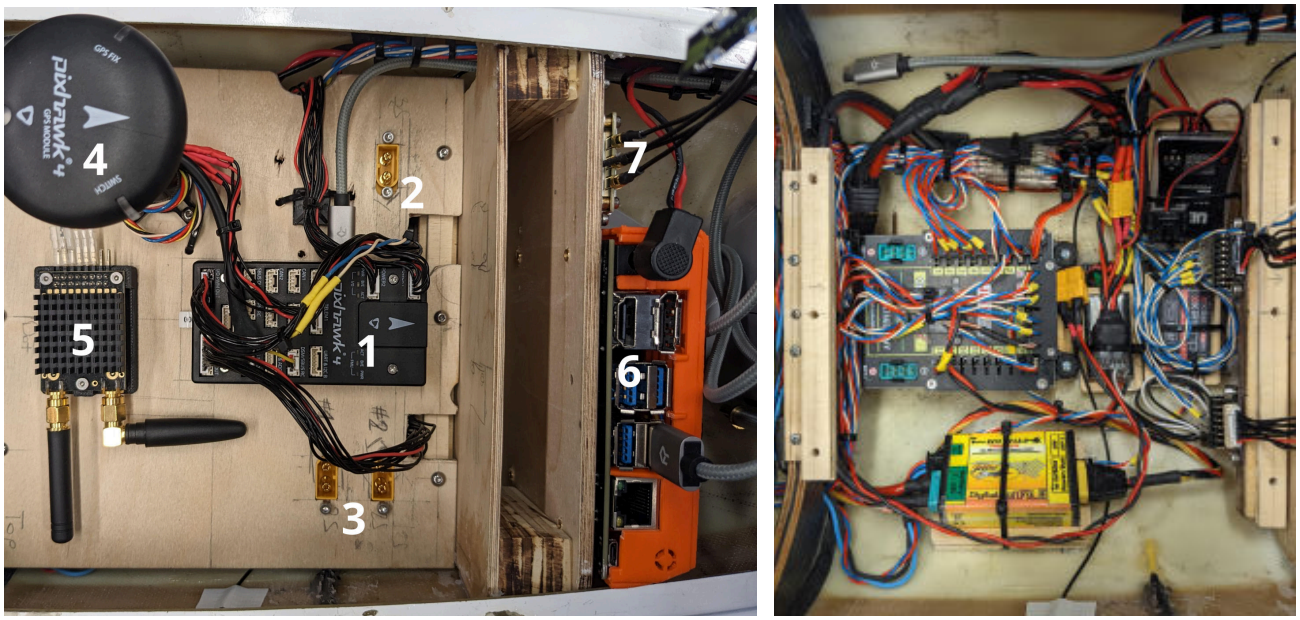

(a) (b)

Figure 6 – Integrated avionics bay with 6a and without 6b the avionics plate during initial range test

To reduce the interference between radio modules, one of the Rex3(RC1) modules are installed in the front section of the fuselage. The Rex3(RC2) and the second RSAT(RC3) modules are installed the middle section of the fuselage under and behind the main fuel-tank, respectively. The two antennas of each module are placed as far as possible from each other with a perpendicular orientation relative to each other. All the antennas were placed directly on the inner side of the fuselage to eliminate local blocking of the radio waves.
The TTS and the OBC was placed in the front section of the fuselage. The TTS is placed in an adjustable height platform, which allows the TTS to be retracted during landing and take-off. A linear motor with end stop detection is used to move the platform. The placement and the retractability of the TTS gave the camera an undisturbed field of view, while keeping a good ground clearance during ground operation.

5.2 System Test Results

During system development, extensive checklists are created for different scenarios like startup, short, and long system tests. Long system tests are used before each test campaign and during

system integration. This covers different edge cases, like loss of battery or RC system connection. System warnings are set and monitored during testing.
Short system tests are used before first operation after assembly for flight. These tests cover telemetry feedback accuracy and synchronization, mechanical connection stability as well as control surface free-play tests.
Startup checklist are used before each operation during system start. Although the system is designed to be non-functional in case of a missing subsystem or wrong initial condition on the RC system, a formality of such procedure ensures full attention and cohesion of the flight test team. During startup, the correctness of major measurements, system controlability and radio quality of the crew is examined before takeoff.
In laboratory conditions as well as during the first flight test campaign most of the integrated subsystems worked as expected.

5.3 Range test results

Two types of range tests are conducted while the system is on the ground. The first, the RC-only, the initial assessment of the quality of the RC antenna placement and expected interference between radios is performed. The second, the drive-away test, is performed to establish the nominal reception quality of all the on board radios. In both cases, the aircraft is fully assembled, with all the subsystems operational. The aircraft is placed in an elevated position relative to the ground.

Figure 7 – Range test configuration

Distance [m]	Jeti [-]	Wi-Fi	RFD 868
10	9	100	25
30	9	100	15
50	9	100	0
125	8	100	0
330	0	0	0
370	5	100	0
420	5	0	0
700	4	0	0
900	3	0	0

Table 7 – Range Test Data Collected on the Ground

During the RC-only test, the transmission power of the RC radio is reduced to 10%. If the pilot can walk 100 meters away from the aircraft without losing connection to the aircraft, the system is deemed good enough to conduct the drive-away test.
During the drive-away test, the pilot and the engineer drive away with the GCS car. During this movement the reception values of the RC system and radio systems are monitored. The telemetry antennas are attached to the extended pole on the GCS similar to the flight test configuration. The transmitter is placed inside the GCS next to the engineer for safety and visibility purposes. The distances and the reception values are recorded periodically. An observer also monitors the response of the aircraft's control surfaces and communicates these with the team in the GCS car.
Figure 7 illustrates the range test configuration along with the prepared ground control station. Table 7 shows the collected data points.
From the three installed JETI receivers, the average of the RC1 and RC2 results are shown. The values of the RC3 module are not presented, as their readings were inconsistent due to the transportation method of the transmitter. In terms of JETI's quality measurement system, 9 indicates good reception and 0 indicates connection lost. The Wi-Fi and the RFD 868 systems indicated values are the reception frequency of the autopilot's attitude information, this data stream was chosen as it is one of the critical higher frequency data streams sent from the autopilot. The nominal values of the Wi-Fi and the RFD 868 system are set to 100Hz and 25Hz respectively.
Table 7 shows reception loss on all subsystems at a distance of 330 meters from the aircraft, and full telemetry loss after 370 meters. At a distance of 330 meters, the Line of Sight (LOS) between the GCS and the aircraft was blocked by the solar panel on the airfield. After a distance of 370 meters,

the LOS is permanently blocked via a tree-line. The RFD 868 module performed less than expected, even within extremely short ranges.

5.4 In-flight range results

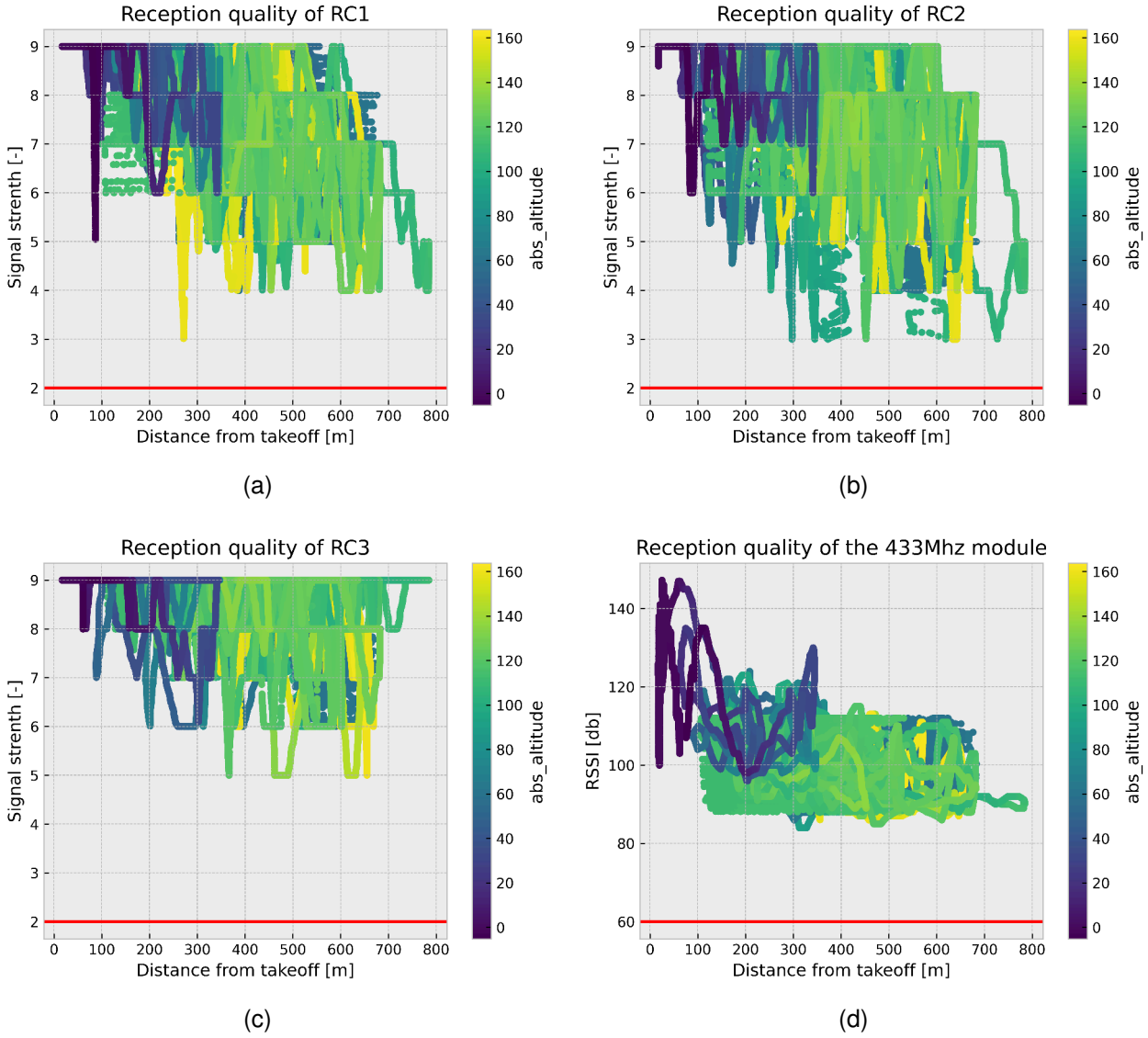

Figure 8 – Radio reception values recorded during fourth flight

Figure 8 shows reception quality measurements recorded during the fourth flight. Similar maps were used after each flight to determine the quality of the radio reception qualities. Only the results from the fourth flight are presented here, due to the highest altitude and distances were measured relative to the GCS during the fourth flight.
The red line on each graph shows a quality limit, under which the radio performance is not acceptable for use. Full reception and control loss for a given radio module happens when the indicated signal strength reaches 0. Even though RC1 and RC2 both have the minimum values at 3, these occured at different points during the flight. That indicates the success of the redundant antenna placement. Figure 8c shows high quality reception values of the RC3 module, which outperforms the main RC modules.
Figure 8d shows RSSI values for the on board 433Mhz radio. The values indicate steady quality, without drastic quality drop. No signal drops were experienced with this system during flight.
During the campaign, there was no quality information collected on the Wi-Fi system. However, in operation it had similar performance as during range test. It worked with close to maximum data

rate as long it had clear LOS and reception. A few data loss event were experienced on the Wi-Fi telemetry. However, in short time the connection was automatically re-established as soon as the aircraft's orientation and position changed such that the antenna was no longer obscured.

5.5 In-flight servo performance

Figure 9a shows the input output performance of flap servos during landing. In both cases, the maximum amplitude matching between the reference signal and the measured servo shaft deflection is not precise. However, the behavior change of the servo motor is observable. Similarly, the airspeed measurements were not properly calibrated, thus the airspeed has an amplitude offset.
The approximate time of landing is indicated via a vertical line at 17.3 minutes. The aircraft becomes stationary after 17.4 minutes. There is a measurable $\sim 0.3°$ difference in the stationary shaft position of the left servo before and after landing. The increased noise on the shaft position measurement between 17.25 and 17.35 minutes comes from the landing impact. A similar phenomena is observable during each landing, only on the left flap. The right flap seems to be able to hold its position.

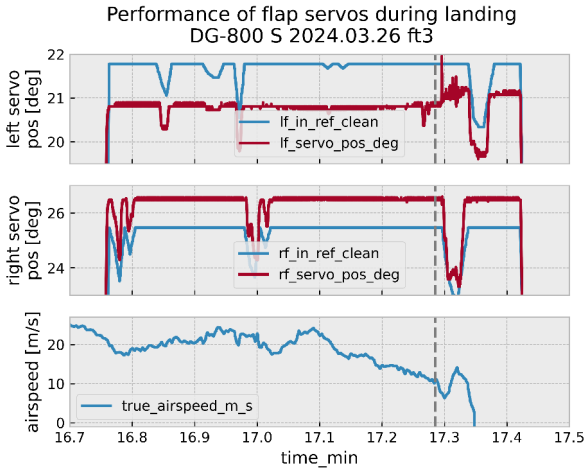

(a) Performance of Flap servos during landing. The dashed line indicated the approximate landing time.

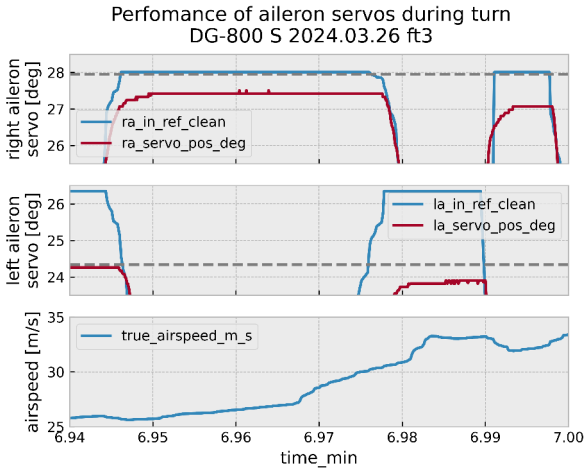

(b) Aileron performance during turn. The dashed lines indicate the nominal deflection in ground.

Figure 9 – Performance degradation of the flap and aileron servos in flight

Figure 9b shows the static performance of the ailerons during a turn. The dashed horizontal lines indicate the maximum measured deflection of the respective servo motor during pre-flight checks.
Based on the collected data, the used servo motor shows two interesting behaviors. First, similarly to the flap servo, it can not reach its nominal maximum deflection over a given hinge-load. This fact is well visible on both servos. Secondly, once the servo reaches a target position, it can hold under smaller load fluctuations. The second fact is observable on the right aileron servo deflection values. Figure 9b indicates different static performance of the left and right aileron servos as well.

6. Discussion

The integration and test results are discussed, and reflected back to the stated requirement list.

6.1 Radio and Telemetry range

The installed JETI system showed more than sufficient performance for safe operation during the range test. The data collected with the Wi-Fi system indicated, that as long as there is clear LOS, the telemetry link is usable. The inadequate range of the RFD 868 module was not investigated further. Instead, due to the interface similarity, it was replaced to a Holybro 433Mhz module [50] with a single dipole antenna. Further range tests were not conducted with the updated control telemetry link, due to previous experience with a similar system configuration.
The conducted range tests were not ideal, due to the following three reasons. Firstly, due to the LOS blocking of the signals by the local solar panels, the tree line and other ground obstacles. Secondly,

the aircraft was stationary with a fixed orientation. Driving in different radius circles or rotating the aircraft would have yielded more realistic results of radio interference and possible orientation problems. Thirdly, it would have been better to carry the RC radio outside of the car, to increase reception on all radios. It was not possible to access the full capabilities of the integrated subsystems. However, given the limitations of the current airfield and requirement from the missions, the system performed well.
The data collected in flight indicates, that the segregated placement of the on board RC antennas caused the worst case points of the RC1 and RC2 modules to occur at different times. The reception quality shown on Fig. 8 indicates, that it would be possible to fly comfortably in an increased flight-box as well.
Some GPS data loss events in flight rendered some interesting artifacts on Fig. 8. Minor data loss events were experienced with the Wi-Fi reception, however it happened only at certain aircraft orientations for the duration of a few seconds. With the 433Mhz system no data loss event is experienced during the flights.

6.2 Actuator Monitoring

The observed performance degradation of the flap and aileron servos with different load cases are an expected result of the ACMU integration. Due to limitation of the ACMU data streaming capabilities at the time, similar effects are only observable after flight on the collected data.
In both cases, the measured performance degradation could be linked to two major factors. Firstly, the torque transfer between the control surface and the servo shaft is not ideal, this could enhance the load experienced by the servo motor. Secondly, the dissimilarity between the individual servo performances can be caused by manufacturing variance.
The connection between the OBC and the ACMUs are not ideal due the rigidity, bulkiness and weight of the USB cables. However, with the integrated USB-Hubs it is possible to add new ACMU modules without changing the existing wiring of the system. Utilizing the Control Area Network (CAN) capabilities of the system, would yield better cabling connections as well as higher data rate.

6.3 System Layout Update

Figure 10 shows the latest version of the avionics plate and the payload area. Changes were made to incorporate the lessons learned from range and flight tests.
The 433Mhz antenna (5) is visible, this was integrated before the flight tests. The GPS (4) antenna holder was replaced by a longer one to reduce the possible interference with the 433 telemetry antenna. The 3S battery plug (2) on the avionics plate was replaced by an XT90 connector from an XT60, to allow dissimilarity between different voltage levels inputs. The original single Wi-Fi antenna (7) was replaced by two separate antenna after the first flight campaign. One is placed alongside the right side of the fuselage, the other is perpendicular to it on the left side of the fuselage. The USB-Hub (9) and the adjustable height platform of the TTS (8) is highlighted as well.

6.4 Reflection on Requirements

The choice of the DG-800 S airframe allows operation on model airfield, and the system design allows easy operation even by a single pilot. The used airframe and system design satisfies Req. 1 and Req. 2. Req. 3 and 4 is satisfied by the use of JETI RC system. Using standard Px4 module along with JETI RC system, Req. 5, Req. 7 and Req. 6 is satisfied. Using a powerful OBC allowed separation of measurements and functionalities required for the autopilot from the measurement required by the authors work, thus satisfying Req. 8. Using the high bandwidth Wi-Fi based telemetry system stratified Req. 9.

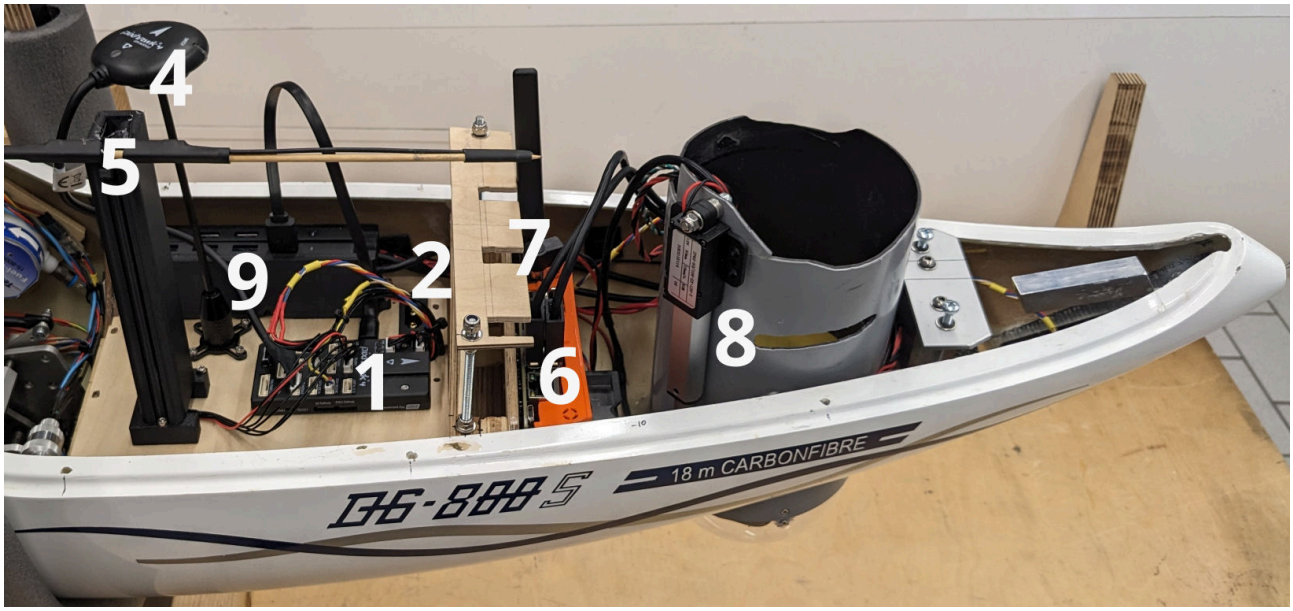

Figure 10 – Updated Payload Area

7. Conclusion

This work described the retrofitting process of the DG-800 S UAV into a multi-purpose test and research platform along with preliminary flight test results. The driving factors for the iterative design are presented as requirements. The selection of the airframe, and the different subsystems is shown along with alternatives. The interconnections and main layout of the subsystems are shown. The connection between main requirements and used subsystems has been highlighted. The integrated systems, in addition to the system and ground based range test results are shown. Radio reception quality, flap and aileron servo performance data is presented from the first flight campaign.
The overall performance of the system is exceptional. Although it has a relatively short flight-time, the good ground handling capabilities allow multiple mission to be flow in short period of time. The well established telemetry and ob-board system support fast feedback on each experiment during operation.
The quality and reception range of the RC and telemetry radios perform well. Based on the collected data, safe operation is expected even with a slightly increased flight operation box. The high update frequency of the streamed data allows timely and precise visual representation of the observed events.
The collected data with the ACMU shows behavioural change of actuator performance under different load situations.
Overall, the quality of the data collected with the system and the operational experience shows that the retrofitting process was successful, thus the need for a high performance research UAV with maximum 25kg has been satisfied.

8. Outlook

Future work includes calibration of different on-board sensors, extensive servo and control surface dynamics identification in flight conditions, improved feedback and data evaluation during missions and live video stream access in the GCS from the on-board camera and a ground based camera system.
As mentioned in [2], additional ACMUs will be installed into the elevator and the rudder servos. In addition to the servo shaft measurements, the elevator will receive two measurement points on the hinge-line. The rudder will receive at least one similar measurement. The results of the additional ACMU integration and calibration are not yet ready at the time of writing.

As mentioned in [2], additional ACMUs were installed into the elevator and the rudder servos. In addition to the servo shaft measurements, the elevator received two measurement points on the hinge-line. The rudder received one similar measurement. The results of the additional ACMU integration were finished after the presented flight test campaign. Calibration and software toolchain integration of these measurement are still on ongoing at the time of writing. Their ground and flight test results, and the analysis of the actuators behaviour response to different identification signals such as used in [2, 14]

9. Acknowledgments

The authors would like to express their gratitude towards Markus Lehmann for his crucial work and assistance on the mechanical integration of the fuselage, and the assistance given during flight test campaign as well as to Thomas Seren for his responsibilities as main pilot of the system and his contribution of the RC system and check list configuration.

10. Contact Author Email Address

Dániel Teubl: daniel.teubl@tum.de
Thando B Sissing: b.sissing@tum.de

11. Copyright Statement

Nomenclature

ACMU Actuator Control and Monitoring Unit

CAN Control Area Network

COTS Commerciall off-the-shelf

ECU Electronic Control Unit

FCC Flight Control Computer

GCS Ground Control Station

GPS Global Positioning System

Graupner Graupner radio System

JETI JETI Model Duplex Radio System

Li Po Lithium polymer

LLS Chair of Aircraft Design

LOS Line of Sight

Lua Lua is a lightweight, embeddable scripting language

MTOW Maximum Take-off Mass

OBC On-Board Computer

PDSA Plan-Do-Study-Act

PowerBox CORE PowerBox CORE Radio System

PWM Pulse Width Modulation

RC Remote Control

REC Rapid Evaluation Class

RFD 868 RFDesign 868Mhz Ultra Long Range Radio Modem [47]

RSSI Received Signal Strength Indicator

SFD Scaled Flight Demonstrator

SNR Signal to Noise Ratio

TTS Target Tracking System

UAV Unmanned Aerial Vehicle

USB Universal Serial Bus

VTOL Vertical Take-off and Landing

Wi-Fi Wireless network protocol based on IEEE.802.11 family of standards.

References

[1] S. J. Koeberle, M. Rumpf, B. Scheufele, and M. Hornung, "Design of a low-cost rpas data acquisition system for education," in *AIAA Aviation 2019 Forum*. American Institute of Aeronautics and Astronautics, 2019. [Online]. Available: https://arc.aiaa.org/doi/10.2514/6.2019-3658

[2] D. Teubl, S. Oberschwendtner, and M. Hornung, *Measurement Results of the ACMU System in Various Research UAVs*. [Online]. Available: https://arc.aiaa.org/doi/abs/10.2514/6.2023-0481

[3] P. Stahl, C. Roessler, and M. Hornung, "Configuration redesign and prototype flight testing of an unmanned fixed- wing evtol aircraft with under-fuselage hover lift and pusher wingtip propulsion system," in *8th Biennial Autonomous VTOL Technical Meeting 6th Annual Electric VTOL Symposium*, 2019. [Online]. Available: https://mediatum.ub.tum.de/node?id=1473755

[4] M. Schmähl, S. Speck, and M. Hornung, "Numeric modeling of the noise emission of a pusher propeller uav configuration," in *AIAA SCITECH 2022 Forum*. American Institute of Aeronautics and Astronautics, 2022. [Online]. Available: https://arc.aiaa.org/doi/10.2514/6.2022-1297

[5] S. J. Koeberle and M. Hornung, "Developments towards a toolchain for uav flight dynamic models in early design." in *32nd Congress of te International Council of Aeronautical Sciences.*, I. S. of the Aeronautical Sciences., Ed., Sep 2021. [Online]. Available: https://www.icas.org/ICAS_ARCHIVE/ICAS2020/data/papers/ICAS2020_0552_paper.pdf

[6] S. J. Koeberle, A. E. Albert, L. H. Nagel, and M. Hornung, "Flight testing for flight dynamics estimation of medium-sized uavs." in *AIAA Scitech 2021 Forum*. American Institute of Aeronautics and Astronautics, 2021. [Online]. Available: https://arc.aiaa.org/doi/10.2514/6.2021-1526

[7] J. Bartasevicius, S. J. Koeberle, D. Teubl, C. Roessler, and M. Hornung, "Flight testing of 65kg t-flex subscale demonstrator," in *32nd Congress of the International Council of the Aeronautical Sciences*, 2021. [Online]. Available: https://www.icas.org/ICAS_ARCHIVE/ICAS2020/data/papers/ICAS2020_0707_paper.pdf

[8] C. Roessler, J. Bartasevicius, S. J. Koeberle, D. Teubl, M. Hornung, Y. M. Meddaikar, J. K. Dillinger, M. Wustenhagen, T. M. Kier, G. Looye, J. Sodja, R. De Breuker, T. Luspay, B. Vanek, P. Georgopoulos, and C. Koimtzoglou, "Results of an aeroelastically tailored wing on the flexop demonstrator aircraft," in *AIAA Scitech 2020 Forum*. American Institute of Aeronautics and Astronautics, 2020. [Online]. Available: https://arc.aiaa.org/doi/10.2514/6.2020-1969

[9] "Flutter free flight envelope expansion for economical performance improvement," Last visited: 2023.10.30. [Online]. Available: https://flexop.eu

[10] "Flight phase adaptive aero-servo-elastic aircraft design methods," Last visited: 2023.10.30. [Online]. Available: https://flipased.eu

[11] J. Schaefer, P. Suh, M. Boucher, J. Ouellette, A. Chin, C. Miller, J. Grauer, G. Reich, R. Mitchell, and P. Flick, "Flying beyond flutter with the x-56a aircraft," 2023. [Online]. Available: https://ntrs.nasa.gov/api/citations/20220012337/downloads/20220012337%20FINAL.pdf

[12] P. Schmollgruber, C. Toussaint, A. Lepage, F. Bremmers, H. Jentink, L. Timmermans, N. Genito, A. Rispoli, D. Meissner, and D. Kierbel, "Validation of scaled flight testing." [Online]. Available: https://www.icas.org/ICAS_ARCHIVE/ICAS2022/data/papers/ICAS2022_0375_paper.pdf

[13] "Carf-models, dg-800 s," Last visited: 2023.11.17. [Online]. Available: https://carf-models.com/en/products/dg-800-s

[14] R. Steffensen, K. Ginnell, and F. Holzapfel, "Practical system identification and incremental control design for a subscale fixed-wing aircraft," *Actuators*, vol. 13, no. 4, 2024. [Online]. Available: https://www.mdpi.com/2076-0825/13/4/130

[15] "Cubepilot cube orange flight controller," accessed: 2023-11-15. [Online]. Available: https://docs.px4.io/main/en/flight_controller/cubepilot_cube_orange.html

[16] "Holybro pixhawk 4," accessed: 2023-11-15. [Online]. Available: https://docs.px4.io/main/en/flight_controller/pixhawk4.html

[17] "Holybro pixhawk 5x," accessed: 2023-11-15. [Online]. Available: https://docs.px4.io/main/en/flight_controller/pixhawk5x.html

[18] "Holybro pixhawk 6c," accessed: 2023-11-15. [Online]. Available: https://docs.px4.io/main/en/flight_controller/pixhawk6c.html

[19] "Sky-drones airlink," accessed: 2023-11-15. [Online]. Available: https://docs.px4.io/main/en/flight_controller/airlink.html

[20] "Ardupilot mega," accessed: 2023-11-15. [Online]. Available: https://www.ardupilot.co.uk

[21] "Openpilot," accessed: 2023-11-15. [Online]. Available: https://librepilot.atlassian.net/wiki/spaces/LPDOC/pages/26968084/OpenPilot+Revolution

[22] "Taulabs sparky2," accessed: 2023-11-15. [Online]. Available: https://ardupilot.org/copter/docs/common-taulabs-sparky2.html

[23] "Powerboc radio system core," accessed: 2024-05-17. [Online]. Available: https://www.powerbox-systems.com/en/products/radio-system/fernsteuersystem/radio-system-core.html

[24] "Jeti dc-16 ii," accessed: 2024-05-17. [Online]. Available: https://www.jetimodel.com/katalog/vysilac-duplex-dc-16-ii-silver-1.htm#product-description-info

[25] "Jeti ds-24," accessed: 2024-05-17. [Online]. Available: https://www.jetimodel.com/katalog/vysilac-duplex-ds-24-.htm#product-description-info

[26] "Frsky taranis seried," accessed: 2024-05-17. [Online]. Available: https://www.frsky-rc.com/product-category/transmitters/taranis-series/

[27] "Lora (short for long range)," accessed: 2024-05-17. [Online]. Available: https://www.semtech.com/lora/what-is-lora

[28] "Frsky tandem seried," accessed: 2024-05-17. [Online]. Available: https://www.frsky-rc.com/product-category/transmitters/tandem-series/

[29] "Expresslrs," accessed: 2024-05-17. [Online]. Available: https://www.expresslrs.org/faq/

[30] "Pixhawk rpi cm4 baseboard," accessed: 2023-11-16. [Online]. Available: https://holybro.com/products/pixhawk-rpi-cm4-baseboard

[31] "Auterion skynode," accessed: 2023-11-16. [Online]. Available: https://auterion.com/product/skynode/

[32] "Raspberry pi 5," accessed: 2023-11-16. [Online]. Available: https://datasheets.raspberrypi.com/rpi5/raspberry-pi-5-product-brief.pdf

[33] "Odroid-m1s with 8gbyte ram + io header," accessed: 2023-11-16. [Online]. Available: https://www.hardkernel.com/shop/odroid-m1s-with-8gbyte-ram-io-header/

[34] "Jetson nano developer kit," accessed: 2023-11-16. [Online]. Available: https://www.nvidia.com/en-us/autonomous-machines/embedded-systems/jetson-nano-developer-kit/

[35] "Jetson agx xavier series," accessed: 2023-11-16. [Online]. Available: https://www.nvidia.com/en-sg/autonomous-machines/embedded-systems/jetson-agx-xavier/

[36] "Optroxa gmb 600," accessed: 2023-11-17. [Online]. Available: https://uxvtechnologies.com/sensors/optroxa-gmb-600/

[37] "Gsg 201," accessed: 2023-11-17. [Online]. Available: https://www.uavos.com/products/gimbals/gsg-201-gimbal/

[38] "2 axis raspberry pi picamera v2 micro brushless camera stabilizer," accessed: 2023-11-17. [Online]. Available: https://www.uavos.com/products/gimbals/gsg-201-gimbal/

[39] "Usg-405," accessed: 2023-11-17. [Online]. Available: https://ukrspecsystems.com/drone-gimbals/usg-405

[40] "Tarot t2-2d brushless 2 achsen gimbal für gopro hero 3 4 -

mod. tl2d01," accessed: 2023-11-17. [Online]. Available: https://www.aerolab.de/tarot-t4-2d-brushless-2-achsen-gimbal-fuer-gopro-hero-3-4-mod-tl2d01_503505_3414

[41] "Siyi a8 4k mini 3 achsen gimbal kamera 6x zoom hdmi ethernet," accessed: 2024-05-20. [Online]. Available: https://www.premium-modellbau.de/siyi-a8-4k-mini-3-achsen-gimbal-kamera-6x-zoom-hdmi-ethernet#

[42] M. Many, M. Weber, S. Oberndorfer, S. J. Koeberle, B. Hosseini, and M. Hornung, "System identification of a turbojet engine using multi-sine inputs in ground testing," in *Deutscher Luft- und Raumfahrtkongress 2021*, D. G. für Luft-und Raumfahrt, Ed., 2021. [Online]. Available: https://www.dglr.de/publikationen/2022/550281.pdf

[43] "Fmsg herrieden stadtel modell airfield," accessed: 2023-11-21. [Online]. Available: https://www.fmsg-herrieden-stadel.de/ueber-uns

[44] "Graupner mc-28 16, 2.4ghz hott radio system, graupner co. ltd." accessed: 2023-11-21. [Online]. Available: https://graupner.com/bbs/board.php?bo_table=a_01&wr_id=6

[45] "Px4," Last visited: 2023.10.30. [Online]. Available: https://docs.px4.io/main/en/

[46] "Ardupilot," Last visited: 2023.10.30. [Online]. Available: https://ardupilot.org/#

[47] "rf design," accessed: 2024-05-21. [Online]. Available: https://rfdesign.com.au/modems/#RFD868x

[48] "Doodle labs nm-db-3 industrial wi-fi transceiver," accessed: 2024-05-21. [Online]. Available: https://techlibrary.doodlelabs.com/nm-db-3-industrial-wi-fi-transceiver-1

[49] D. Teubl, T. Bitenc, and M. Hornung, "Design and development of an actuator control and monitoring unit for small and medium size research uavs," *Deutsche Gesellschaft für Luft- und Raumfahrt - Lilienthal-Oberth e.V.*, 2021. [Online]. Available: https://www.dglr.de/publikationen/2021/550036.pdf

[50] "Holybro telemetry radio," accessed: 2024-05-21. [Online]. Available: https://docs.px4.io/main/en/telemetry/holybro_sik_radio.html

[51] "Spektrum dsm," accessed: 2024-05-21. [Online]. Available: https://www.spektrumrc.com/spm-bs-dsmr.html